Estimation of Dosimetric Parameters based on K_{NR} and K_{NCSF} Correction Factors for Small Field Radiation Therapy at 6 and 18 MV Linac Energies using Monte Carlo Simulation Methods

Rahimi S. A.[1,4], Hashemi B.[2]*, Mahdavi S. R.[3]

[1]PhD Candidate, Department of Medical Physics, Faculty of Medical Sciences, Tarbiat Modares University, Tehran, Iran
[2]Associate Professor, Department of Medical Physics, Faculty of Medical Sciences, Tarbiat Modares University, Tehran, Iran
[3]Associate Professor, Department of Medical Physics, Faculty of Medicine, Iran University of Medical Sciences, Tehran, Iran
[4]Assistant Professor, Department of Basic Sciences, Faculty of Health Sciences, Mazandaran University of Medical Sciences, Sari, Iran

ABSTRACT

Background: Estimating dosimetric parameters for small fields under non-reference conditions leads to significant errors if done based on conventional protocols used for large fields in reference conditions. Hence, further correction factors have been introduced to take into account the influence of spectral quality changes when various detectors are used in non-reference conditions at different depths and field sizes.

Objective: Determining correction factors (K_{NR} and K_{NCSF}) recommended recently for small field dosimetry formalism by American Association of Physicists in Medicine (AAPM) for different detectors at 6 and 18 MV photon beams.

Methods: EGSnrc Monte Carlo code was used to calculate the doses measured with different detectors located in a slab phantom and the recommended K_{NR} and K_{NCSF} correction factors for various circular small field sizes ranging from 5-30 mm diameters. K_{NR} and K_{NCSF} correction factors were determined for different active detectors (a pinpoint chamber, EDP-20 and EDP-10 diodes) in a homogeneous phantom irradiated to 6 and 18 MV photon beams of a Varian linac (2100C/D).

Results: K_{NR} correction factor estimated for the highest small circular field size of 30 mm diameter for the pinpoint chamber, EDP-20 and EDP-10 diodes were 0.993, 1.020 and 1.054; and 0.992, 1.054 and 1.005 for the 6 and 18 MV beams, respectively. The K_{NCSF} correction factor estimated for the lowest circular field size of 5 mm for the pinpoint chamber, EDP-20 and EDP-10 diodes were 0.994, 1.023, and 1.040; and 1.000, 1.014, and 1.022 for the 6 and 18 MV photon beams, respectively.

Conclusion: Comparing the results obtained for the detectors used in this study reveals that the unshielded diodes (EDP-20 and EDP-10) can confidently be recommended for small field dosimetry as their correction factors (K_{NR} and K_{NCSF}) was close to 1.0 for all small field sizes investigated and are mainly independent from the electron beam spot size.

Keywords

Small field radiotherapy, Correction factors, TG155, Monte Carlo, Pinpoint chamber, Diode dosimeter

Introduction

Novel radiotherapy techniques are continuously developing. In this regard, radiation field sizes smaller than conventional dimensions are getting used to deliver higher gradient radia-

*Corresponding author: B. Hashemi
Department of Medical Physics, Faculty of Medical Sciences, Tarbiat Modares University, Al-Ahmad and Chamran Cross, P.O.Box: 14115-111, Tehran 1411713116, Iran.
E-mail: bhashemi@modares.ac.ir

Received: 24 July 2015
Accepted: 24 Decdmber 2016

tion doses to patients [1, 2]. For high precision in some novel radiotherapy practices such as intensity modulated radiotherapy (IMRT) and stereotactic radiosurgery, it is fundamental to determine the doses for small photon fields with a high accuracy. However, the accuracy of experimental dosimetry for small fields is limited due to the lack of lateral charge particle equilibrium, spectral changes as a function of field size, sensitivity variations of the detectors used and the non-negligible volume of detectors [3, 4]. On the other hand, all common dosimetry protocols are based on the measurements made under reference conditions [5, 6]. In such protocols, field sizes are usually normalized to the reference field size of 10×10 cm^2 as standard. However, the accuracy and precision of dosimetric measurements in phantoms largely depend on the detectors used, diverse perturbation effects due to the presence of the detector in the medium, as well as deviations from calibration conditions [3, 4].

In common dosimetry protocol (based on either TRS398 [5] or TG51 [6]), the dose to water $(D_{(w,Qmsr)}^{(f_{msr})})$ is calculated by using Equation 1 for a small cylindrical shape of water (where the measuring chamber is located) in standard reference condition, while the dose to a PMMA phantom in non-reference conditions (small fields) $(D_{(m,Qmsr)}^{(f_{msr})})$ is calculated by Equation 2 for a PMMA voxel having a radius of 0.1 mm and a height of 1 mm [4-6].

$$D_{w,Qmsr}^{f_{msr}} = M_{Q_{msr}}^{f_{msr}} . N_{Dw,Q_0} . K_{Q,Q_0} \quad (1)$$

$$D_{m,Qmsr}^{f_{msr}} = M_{Q_{msr}}^{f_{msr}} . N_{Dw,Q_0} . K_{Q,Q_0} . k_{Q_{msr},q}^{f_{msr},fref} \quad (2)$$

In these equations $M_{Q_{msr}}^{f_{msr}}$, K_{Q,Q_0}, and N_{Dw,Q_0} are the chamber reading, its calibration factor, and the radiation quality factor at the standard reference condition, while $k_{Q_{msr},q}^{f_{msr},fref}$ is an extra radiation quality factor proposed to be used for non-reference (small fields) conditions.

Based on some preliminary calculations, it has been stated [7] that a further decrease in the voxel size will not change the dose to the voxel within the acceptable uncertainty limits (<0.2%), even for the smallest field size, i.e. the volume averaging for the voxel size is claimed to be negligible. However, a common effect of non-water equivalent radiation detectors intended for measuring the absorbed dose to water, compared with the ideal small water-equivalent probe, is their over- or under-response to the photon fields with different amounts of low-energy photons [8]. Thus, the response is defined as the quotient of the detector signal and the absorbed dose to water in the undisturbed medium at the position of an effective measurement point of the detector. Although spatially highly resolved measurements are achievable with some detectors such as radiographic films, thermoluminescent detectors and Si diodes, their over- or under-responses render them error-prone when applied in photon beams having radiation qualities different from that used in their calibration procedure [6, 7].

Hence, Alfonso et al [9] proposed a new formalism for the small and non-standard field dosimetry procedures, introducing a new detector-dependent correction factor which may be determined only by Monte Carlo simulations [3, 4]. In several publications, correction factors or different notation of factors have been provided for various detectors in small radiation fields for several linacs [7, 9, 10].

To overcome the problems encountered due to the variation of beam qualities and energy spectra in small field radiotherapy compared to conventional radiation field sizes, a new protocol has been recommended by a task group of AAPM [11] (TG155) to determine some correction factors required for such small field sizes. The recommended correction factors take into account the probable variation caused by the dosimeter response at the reference and non-reference conditions and increase the level of precision of experimental

dosimetry procedures for small field sizes [5, 6, 11].

Due to the variation of radiation quality in small field radiotherapy and the lack of precise knowledge and information on the correction factors proposed for such fields and the effect of these factors on related dosimetry parameters, the recommended TG155 correction factors [11] have to be determined. TG155 recommends the application of further correction factors including the non-reference condition correction factors of K_{NR} (Non-reference condition correction factor), K_{NCSF} (Non-reference small field condition correction factor) to take into account the possible changes of the detector response under non-reference conditions. By definition, the correction factor is unity under reference conditions and deviates from unity in non-reference conditions. The TG155 correction factors (K_{NR}, K_{NCSF}) recommended for non-reference conditions were calculated in this study by using Monte Carlo calculations as well as experimental measurements for four small field sizes based on the novel protocol proposed by the AAPM task group [11], the formalism proposed by Alfonso et al. [9], and other previous studies made on small field dosimetry based on Monte Carlo calculations [12-14]. Our calculations/measurements were performed at 6 and 18 MV energies produced by a Varian Oncology Systems clinic linac (2100C/D) for three different ionizing detectors including a pinpoint chamber and two different diodes. In addition, experimental measurements were performed to estimate the electron beam spot size of the linac via comparing the experimental and simulated data.

Material and Methods

Measurements

Radiation Source and Field Definitions

All experimental measurements were made at the radiotherapy department of Pars Hospital in Tehran/Iran. A Varian Oncology System clinic linac (2100C/D) equipped with small field collimators was used to deliver 6 and 18 MV photon beam energies.

Small Field Collimators

Various small field sizes (including 5, 10, 20 and 30 mm) were defined by using separate circular collimators. In this regard, the external home-made small field collimators were attached to the linac.

Detectors

Three Scanditronix p-type diodes (Germany) including an EPD-10, EPD-15 and EPD-20 recommended for in-vivo dosimetry of high energy photon beams were used. These detectors are designed to facilitate the implementation of a fast and accurate in-vivo dosimetry routinely. In addition to the diode dosimetry system, a pinpoint chamber having a 100 nC/Gy Typical sensitivity (PTW31006, Germany) and EBT2 films were used based on the protocol recommended and described in the TG155 report [11]. Table 1 shows the characteristics

Table 1: Characteristics of Scanditronix Diodes

Detector	Applications, build-up	Water equivalent	Sensitivity decrease at 250 Gy
EDP-10 (green)	4-8 MV (photons,) entrance dose, few corrections, exit dose	10 mm	≥%1 (less than the mass accuracy) at 6 MV
EDP-15 (red)	6-14 MV (photons) entrance dose, few corrections, exit dose	15 mm	≥%1 (less than the mass accuracy) at 6 MV
EDP-20 (yellow)	8-18 MV(photons,) entrance dose, few corrections, exit dose	20 mm	≥%1 at 1 MV

of the Scanditronix diodes used in this study.

Measurement Setup

High-energy photon beams were directed vertically down into a 30×30×30 cm^3 water tank phantom and a slab phantom equipped with a vertical translation stage centered on one of the slabs positioned appropriately beyond the buildup region for 6 and 18 MV photon energies. The detectors were attached to the linac head by means of acrylic holders so that they are fixed vertically along the secondary collimators under the linac treatment head. The SSD was set at 100 cm and the detectors were positioned at the beam isocenter at a known depth in the water phantom. For the ionization chamber setup, the point of measurement was set at 10 cm depth in the water phantom but for the diode set up this point was set at 5 cm depth in the slab phantom [13, 14].

Correction Calibration of Diodes

The correction calibration is a complement to the sensitivity calibration of diodes that takes care of the difference in the detector response from that expected to the actual reading value. This correction factor is used to correct the detector response due to other specific (small) field sizes, SSDs, wedges, etc. to its common known normalized standard setup (made at 10×10 cm^2 field size and SSD=100 cm). This correction factor will differ slightly from 1.00. Furthermore, if diodes had been in use since their last sensitivity calibration, extra recalibration must be done prior to the specific correction calibration. Extra correction factors are required to be made for different treatment set-ups (field sizes, SSDs, wedges) for several reasons. One reason is that diodes are not ideal. But, the main reason is that in in-vivo dosimetry when the dose is measured at the point of interest, the skin of the patient does not change proportionally to the dose at the D_{max} for different set-ups. This mainly depends on the larger contribution of secondary electrons at the skin of the patient than that at the D_{max}. The good point is that the relation between the correction factors would be constant if a high quality detector is used whereby it needs to be measured normally just once. Figure 1 shows the diode calibration procedure made for entrance dose measurements.

Irradiation

All experimental measurements performed for the detectors were made by using the 6 and 18 MV photon beams of the Varian linac. The homogeneous phantom used in the study (a PMMA phantom) was irradiated to 6 and 18 MV linac energies at various circular small field sizes of interest (with 5, 10, 20 and 30 mm diameters). The dosimetry procedures were made with a pinpoint chamber and three types of diodes (EDP-20, EDP-15 and EDP-10) separately by placing several layers of

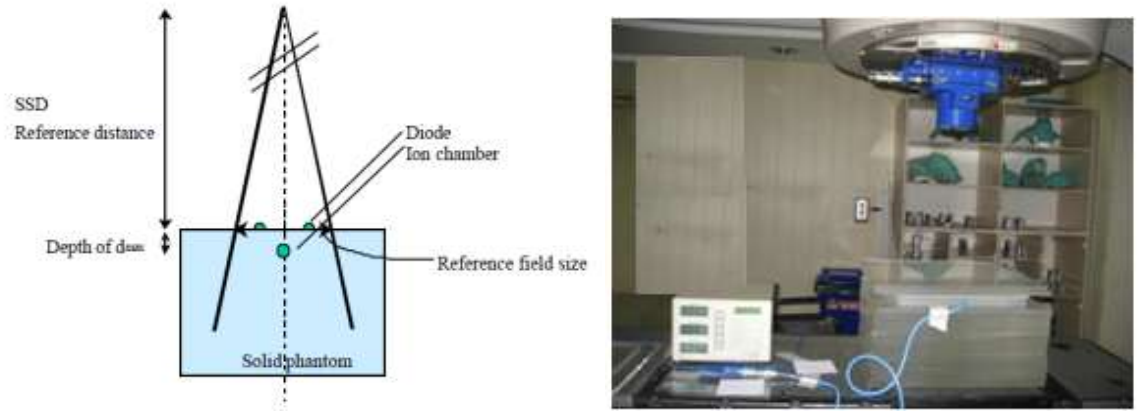

Figure 1: Diode calibration procedure for entrance dose measurements. The ionization chamber is positioned at the reference depth in the phantom and the diode at the entrance surface in the reference geometry.

similar thicknesses of the slab phantom as required for each circular small field size. To ensure the accuracy/reliability of the measurements, each measurement was repeated three times from which the average was calculated and used. The results measured experimentally from irradiating the homogeneous phantom were compared with those obtained from the Monte Carlo calculations.

Monte Carlo Simulations

Validation of Linac Nominal Energies for Monte Carlo Simulations

To validate the calculated photon beams produced by Monte Carlo simulations for the Varian linac, the calculated photon spectra and dose distributions were compared with those measured experimentally with the pinpoint chamber. Several electron energies were simulated including 5.8, 6.0, and 6.2 MV; and 17.8, 18.0, and 18.2 MV for the nominal 6 and 18 MV energies, respectively. In this regard, the calculated PDDs were compared with the standard experimental measurements made for 6 and 18 MV nominal energies. The best matching of the assumed electron energies was chosen when the sum of the differences of the calculations made by MC simulations relative to the experimental measurements indicated the lowest values for the distance to agreement (DTA) and local dose difference (DD) parameters. As could be noted from the data presented in Table 2, the best matching energies for the nominal 6 and 18 MV energies of the linac have been 6.2 and 18.0 MV indicating less than 1% error being less than all other energies.

Table 2: Comparing different parameters determined with the experimental measurements and Monte Carlo calculations at 6 and 18 MV photon energies

Energy (MeV)	FWHM (mm)	DTA (mm) (mean ± SD)	DD (%) (mean ± SD)
18	0.15	0.59 ± 0.38	0.53 ± 0.48
6.2	0.20	0.24 ± 0.17	0.45 ± 0.33

Monte Carlo Simulations

Monte Carlo simulations were carried out by using BEAMnrc and DOSXYZnrc codes for all the required dose calculations. Both of these codes are based on an electron gamma shower user code (EGSnrc) that comes as a package under the license of the National Research Council of Canada [7, 10, 15]. The Varian linac (Varian Oncology Systems, 2100 C/D) head geometry was modeled by the BEAMnrc [15]. All the materials and the structure of the linac head were defined based on the specifications provided by Varian Company.

The BEAMnrc simulations were performed with an energy threshold of ECUT=0.07 MeV for electrons as well as positrons and PCUT=0.01 MeV for photons [16-18]. A total of 3×10^9 and 10^9 histories were studied for the accelerator head calculations for the 6 and 18 MV energies respectively.

To improve the efficiency of Monte Carlo simulations, the variance reduction technique of directional Bremsstrahlung Splitting (DBS) was used [15]. For the linear accelerator geometry, a splitting number of 1000 and 750 was selected for optimal simulation efficiency at 6 and 18 MV energies, respectively [7, 12]. According to Kawrakow et al recommendation [16, 17], a splitting field radius of 10 cm at a distance of 100 cm from the source was chosen for the 10×10 cm^2 reference field. For other field sizes, the splitting radius was set equal to the side length of the radiation field (e.g. a splitting field radius of 3 cm at a distance of 100 cm from the source was chosen for the 30 mm cone size) [16, 17].

The primary output of the BEAMnrc simulation for the head of the linac is a file called phase space file (PHSP) having the information about all the particles leaving the accelerator. This file was scored in a plane perpendicular to the beam axis at 100 cm distance from the target. To model the initial electron beam in the treatment head, the BEAMnrc source ISOURCE=19 was used. The phase

space files were generated with BEAMnrc for different field sizes and electron beam spot sizes. The circular field sizes varied from 5 to 30 mm and the initial electron beam spot size FWHM from 1.3 to 1.8 mm [17, 18]. The user code BEAMDP (BEAM utility program) was used to calculate the photon flounce from PHSP files created at a depth of 4 cm in the PMMA phantom [17].

The BEAMDP program was used to read and process the data in the PHSP files and plot the energy spectra of the photon beams. To validate the Monte Carlo model for the photon-beam output of the Varian linac, four PHSP files were created for the 5, 10, 20 and 30 mm circular field sizes and the standard 10×10 cm^2 square field size, at every 2 cm in the PMMA phantom [12, 14]. The resulting 112 PHSP files were used as the input files for DOSXYZnrc code to determine the dose distribution in the perspex (PMMA) phantom created by this program. The PMMA phantom was created by using the DOSXYZnrc code. The voxel size used to calculate the dose was 0.25 mm in the direction of measurement and 1.0 mm in the other two dimensions [4, 8, 9, 12].

The PMMA phantom was located at a source-to-surface distance (SSD) of 100 cm. These 112 PHSP files (one phase space file for every 2 cm) in the perspex phantom (having a depth of 28 cm for both of the 6 and 18 MV energies) were used as the input file for BEAMDP simulation program to determine the photon energy fluence spectra distribution in the perspex phantom created by DOSXYZnrc program. Figure 2 shows the geometry of the phantom used to model the diode detector in the PMMA medium using DOSXYZnrc in this study.

The dose within the sensitive volume of three different types of detectors (Table 1) was calculated with the user code of "egschamber" [19, 20]. The detector geometries were modeled in detail according to the information given by the manufacturer (Scanditronix, Germany) using the user code of geometry

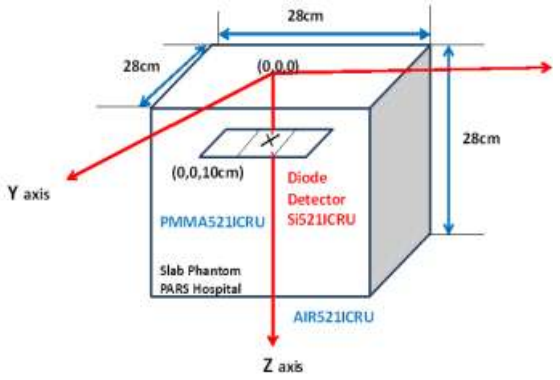

Figure 2: The phantom used to model the diode detector in the PMMA medium using DOSXYZnrc MC code.

package [21, 22]. The ionization chamber was modeled including all the details such as its central electrode, stem and capsule. The diode detectors were modeled including their whole silicon chip and surrounding material.

Non-reference Condition Correction Factors, K_{NR} and K_{NCSF}

The K_{NR} factor shall compensate for the change of the detector response in non-reference $Y_t(x)$ compared to the reference $Y_t(x_{ref})$ condition [8, 23, 24] as expressed in the following equation:

$$K_{NR} = Y_t(x_{ref})/Y_t(x) \qquad (3)$$

in which, X_{ref} and x represent the reference and non-reference conditions, respectively. Thus, if $Y_t(x)$ is larger than $Y_t(X_{ref})$, e.g. in the well-known case of over response of p-type diodes in the periphery of a phantom field where low energy scattered radiation dominates, the K_{NR} would be smaller than unity [8]. The non-reference detector response $Y_t(x)$ is obtained from a formula suggested by Wulff et al. [8, 12] as follows:

$$Yt(x) = \frac{\sum_{i=1}^{n} r_t(E_i)\left[\frac{\mu_{en(E_i)}}{\rho}\right]_m \varphi_{E_{Non-reference}}(E_i)E_i\Delta E_i}{\sum_{i=1}^{n}\left[\frac{\mu_{en(E_i)}}{\rho}\right]_w \varphi_{E_{Non-reference}}(E_i)E_i\Delta E_i} \quad ....(4)$$

The details of the parameters used in this equation are described in Table 3. In this table the detector response parameters used in Equation 4 for determining $Y_t(x)$ are shown [8, 12]. The $r_t(E_i)$ introduced in the table is the response of the detector type t, defined as the quotient of the detector signal and the absorbed dose to water at the point of measurement, to mono-energetic photons of energy E_i under the same conditions of use, such as the PMMA case for the set of EDP diodes, under which the detector is applied for the high energy photon beams. The $r_t(E_i)$ values for the pinpoint chamber and unshielded Scanditronix diodes (EDP-10 and EDP-20) were measured and validated with those reported by Wulff [12] and Edwards [25] from Monte Carlo calculations [11]. The factor $\left[\frac{\mu_{en}(E_i)}{\rho}\right]_m$ is the mass energy absorption coefficient of water and PMMA and $\varphi_E(E_i)$ the spectral photon fluence at energy E_i [24]. The photon fluence spectra $\varphi_E(E_i)$ values needed to be used in Equation 4 were determined by Monte Carlo simulations [8, 18, 24]. The head structure of the Varian linac operating at nominal voltages of 6 and 18 MV was utilized. By using the calculated energy spectra, the response for each detector was achieved. The first necessary step was to calculate the values of the spectrum-weighted response for the reference and general conditions, $Y_t(x_{ref})$ and $Y_t(x)$. According to Equation 4, it was required to calculate the photon spectra under various conditions in- and outside the geometric field limits.

The K_{NR} for the small circular fields (with 30 mm diameter) were measured experimentally at various depths by using Equations 3 and 4 for the 6 and 18 MV energies.

In small field dosimetry, where a small field size of 4×4 cm^2 is used as the reference, the associated non-reference condition factor is termed as the K_{NCSF}. This factor is determined from the following equation:

$$K_{NCSF} = Y_t(x_{cal,SF})/Y_t(x) \quad (5)$$

where $x_{cal,SF}$ represents the conditions of the small calibration field and x the general conditions. The conversion from the correction factor of K_{NR} to K_{NCSF} for any given condition x is given by combining Equation 3 and 5, through the following equation:

$$K_{NCSF}(x) = K_{NR}(x)/K_{NR}(x_{cal,SF}) \quad (6)$$

The K_{NCSF} for the small circular fields (with 5 and 10 mm diameters) were measured experimentally at various depths by using Equa-

Table 3: Non-reference Detector Response $Y_t(x)$ Parameters

$r_t(E_i)$ Response of detector type t	Response of detector at 6 MV energy in PMMA phantom for the diodes (EDP-10 and EDP-20) and Pinpoint dosimeters	Response of detector at 18 MV energy in PMMA phantom for the diodes (EDP-10 and EDP-20) and Pinpoint dosimeters
$\left[\frac{\mu_{en(E_i)}}{\rho}\right]_w, \left[\frac{\mu_{en(E_i)}}{\rho}\right]_m$	Mass energy absorption coefficient of water and PMMA	Mass energy absorption coefficient of water
$\Phi_E(E_i)$ Non-reference	Spectral photon fluence at 6 MV energy (E±ΔE = 6±%20)	Spectral photon fluence at 18 MV energy (E ± ΔE = 18 ±%20)
ΔE_i constant bin width	10 KeV	24 KeV
$(\mu_{en}/\rho)_w \Phi(E_i)\, E_i \Delta E_i$ Non-reference	Absorbed dose to water(and PMMA) at the energy interval ΔE_i (10 KeV)	Absorbed dose to water(and PMMA) at the energy interval ΔE_i (24 KeV)

tion 6 for the 6 and 18 MV energies.

Calculating K_{NR} and K_{NCSF}

The values of K_{NR} and K_{NCSF} were calculated according to Equations 3, 4 and 5. Generally, the deviations of K_{NR} from unity for all the depths and field sizes were smaller for the 18 MV beam compared to the same conditions for the 6 MV beam due to the smaller spectral contribution of low-energy photons at 18 MV.

Results and Discussions

Some spectra calculated by BEAMDP program for the 6 and 18 MV incident plane parallel beams are plotted in Figures 3-5 for circular field sizes of 5, 10, 20, and 30 mm diameters and also the reference square field size of 10×10 cm^2. All the spectra were calculated for different field sizes at 10 cm depth on the central axis. The spikes observed in some of the spectra are due to a discretization effect of the larger scored energy bin width of the scattered photons compared to the primary incident photons. It has already been concluded by Eklund and Ahnesjö [24] that the discretization effect does not introduce any errors in the calculated spectra. For the small field sizes investigated in this study, the scattered component is negligible [24, 26, 27]. Therefore, this component was not considered in the MC simulations. Based on international codes of practice for clinical high-energy photon beam

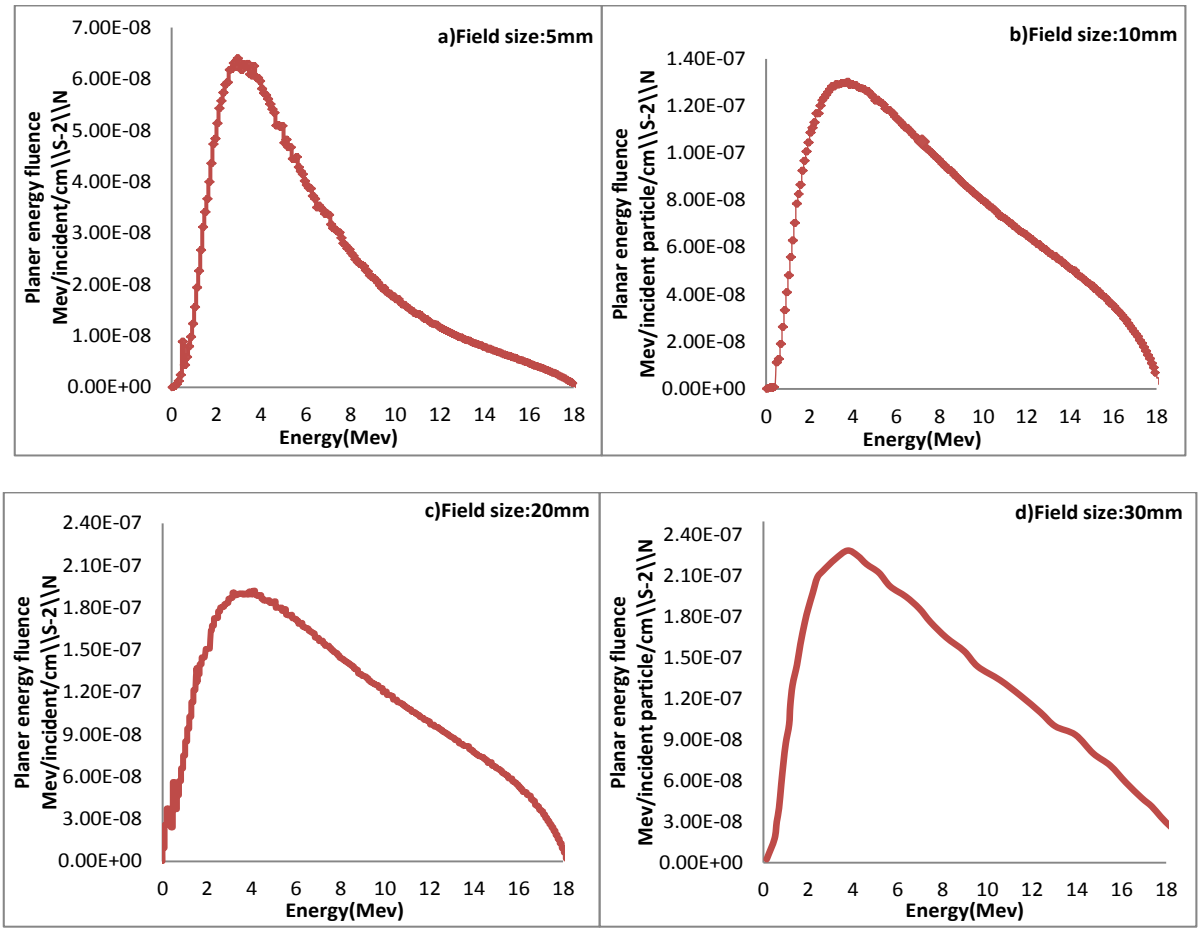

Figure 3: Photon energy fluence spectra of 18 MV photon beam calculated at 10 cm depth on the central axis for various circular small field sizes, a: 5, b: 10, c: 20, d: 30 mm diameter. The plotted spectra are normalized to the total incident photon energy fluence ϕ_0 by using Equation (4).

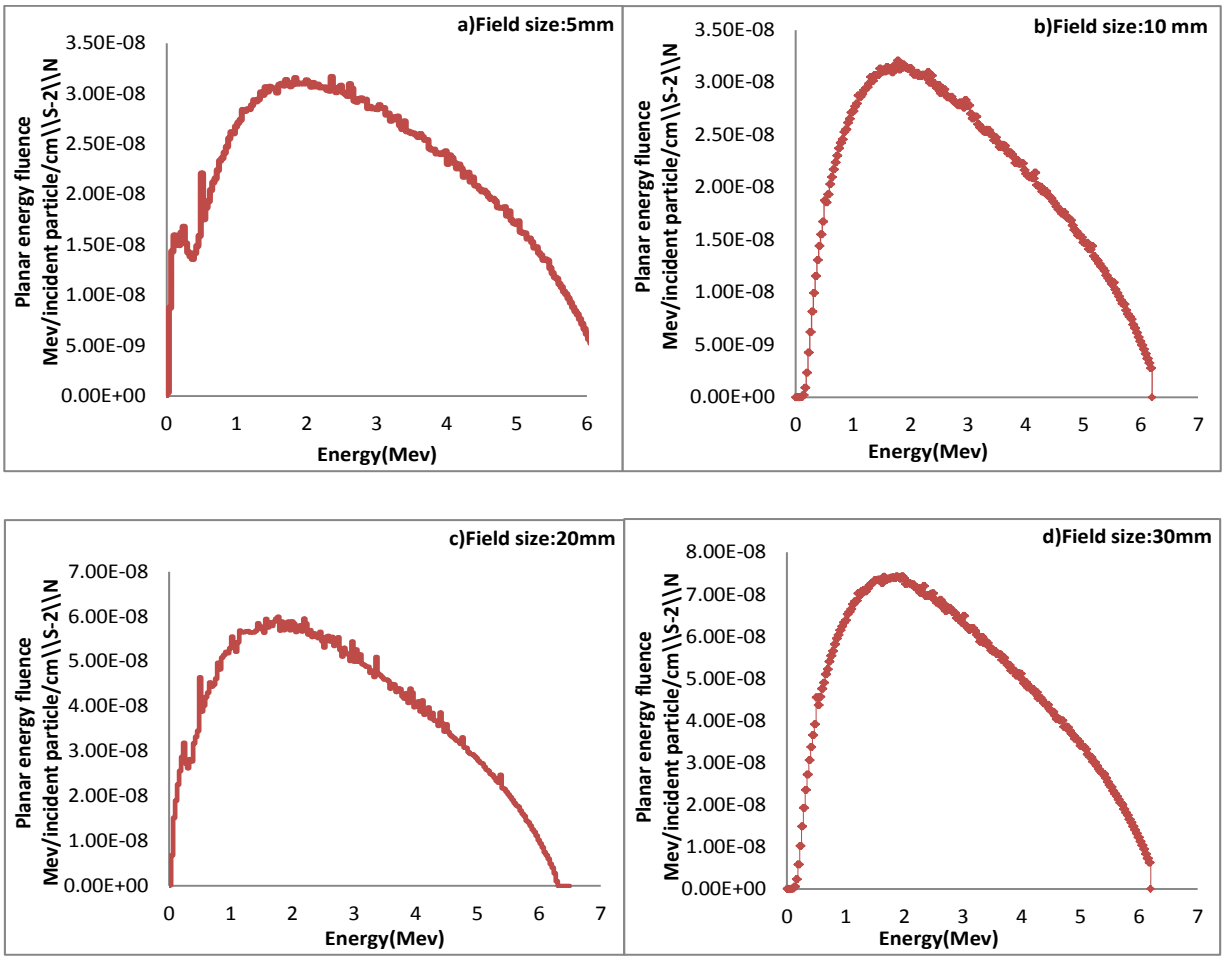

Figure 4: Photon energy fluence spectra of 6 MV photon beam calculated at 10 cm depth on the central axis for various circular small field sizes, a: 5, b: 10, c: 20, d: 30 mm diameter. The plotted spectra are normalized to the total incident photon energy fluence ϕ_0 by using Equation (4).

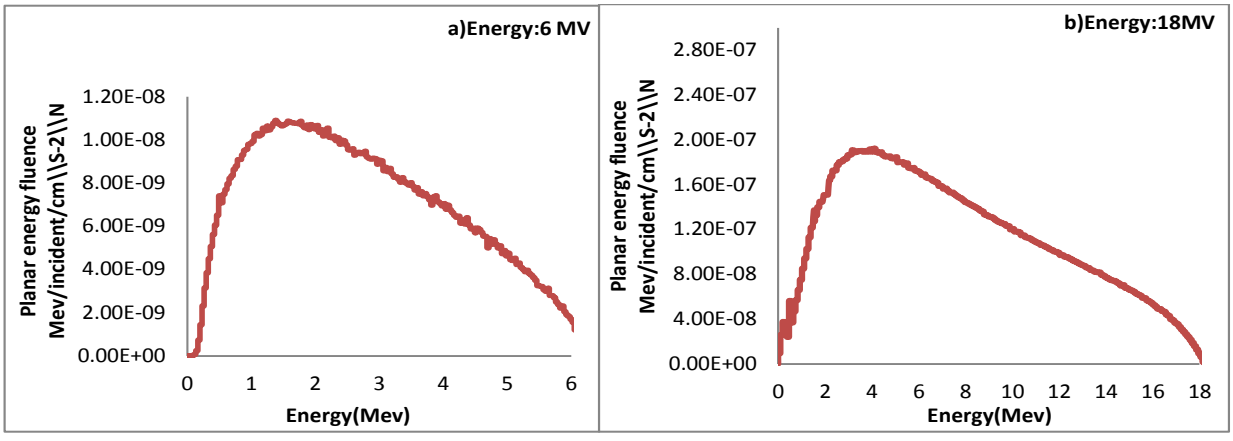

Figure 5: Photon energy fluence spectra for the reference 10×10 cm^2 field size at 10 cm depth on the central axis, for the 6 (a) and 18 (b) MV photon beams. The plotted spectra are normalized to the total incident photon energy fluence ϕ_0 by using Equation (4).

dosimetry [28], the quality factor K_Q only corrects the calibration factors of various dosimetric detectors as far as the detectors are used under reference condition and further correction factors, K_{NR} and K_{NCSF}, are needed to correct for the changes of detectors' response occurred in non-reference conditions. The K_{NR} and K_{NCSF} calculated in this study were based on the detector responses for mono-energetic photons [8, 23, 24]. The K_{NR} and K_{NCSF} values were calculated according to Equations 3, 4 and 5 for various dosimeters (EDP diodes and Pinpoint chamber). Figures 6-9 show the depth dependence of the non-reference condition correction factor (K_{NR} and K_{NCSF}) for various detectors at various points on the central beam axis at 6 and 18 MV photon beams for various field sizes. For the points of interest on the beam central axis using the 10×10 cm^2 field size at 10 cm depth as the reference field, both K_{NR} and K_{NCSF} correction factors will be equal to 1.00 [23, 24]. The deviations of the non-reference condition correction factors of K_{NR} and K_{NCSF} from unity can be used to provide more accurate photon beam dosimetry in the phantoms under specific conditions of depths and field sizes different from the reference condition.

Table 4 shows the calculated values of K_{NR}

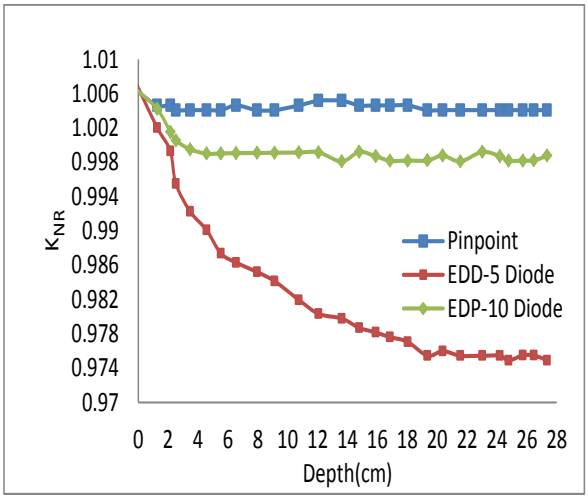

Figure 7: Depth dependence of the non-reference condition correction factor (K_{NCSF}) for various detectors at various points on the central beam axis at 18 MV photon beam for the circular 30 mm field size in the phantom defined by Equation (3).

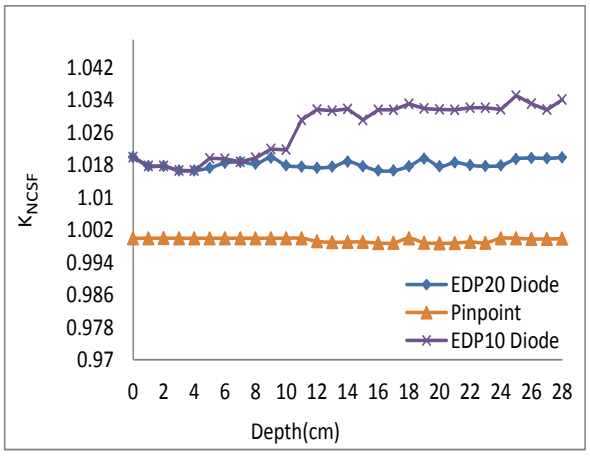

Figure 6: Depth dependence of the non-reference condition correction factor (K_{NCSF}) for various detectors at various points on the central beam axis at 18 MV photon beam for the circular 5 mm diameter field size in the phantom defined by Equation (5).

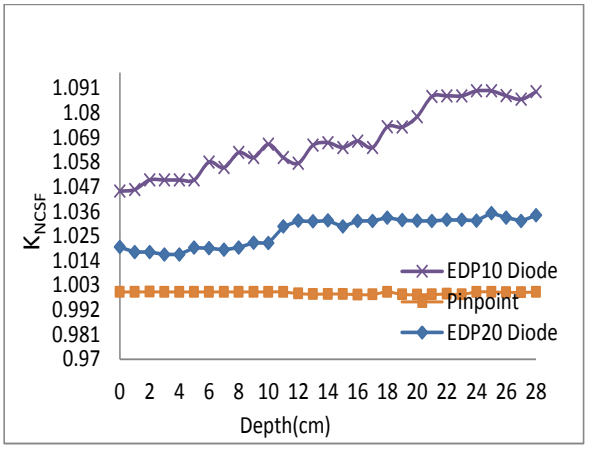

Figure 8: Depth dependence of the non-reference condition correction factor (K_{NCSF}) for various detectors at various points on the central beam axis at 6 MV photon beam for the circular 5 mm field size in the phantom defined by Equation (5).

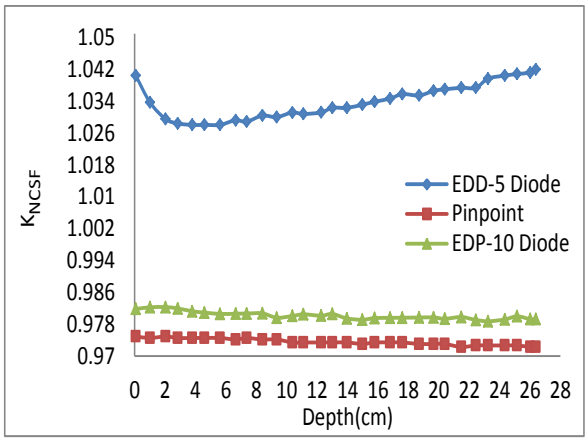

Figure 9: Depth dependence of the non-reference condition correction factor (K_{NCSF}) for various detectors at various points on the central beam axis at 6 MV photon beam for the circular 10 mm field size in the phantom defined by Equation (5).

(X_{cal}, SF) for the 6 and 18 MV photon energies and various radiation detectors at 10 cm depth of the homogeneous phantom shown in Figure 1. The accuracy of the K_{NR} and K_{NCSF} values depend on the accuracy of the input values, i.e. the energy dependent responses $r_t(E_i)$ of various detectors for mono-energetic photons as seen in Table 4. These uncertainties are detector dependent, and according to Equation 4 they will appear practically unmodified in the K_{NR} values. Thus, we estimated the deviations of the K_{NR} values from unity to have uncertainties of the order of 5%. The second source of numerical uncertainties comes from the Monte Carlo derived photon spectra, serving as the input to Equation 4 [8, 22, 23].

Table 4: Values of K_{NR} derived from Equation 3 for various detectors at 10 cm depth of the phantom for the circular 30 mm diameter field size.

Detector type	6 MV	18 MV
Pinpoint	0.998	0.997
Diode EDP-10	1.004	1.002
Diode EDP-15	1.008	1.003
Diode EDP-20	0.993	0.997

Generally, the deviations of K_{NR} from unity for all depths and field sizes were smaller for the 18 MV compared to 6 MV that can be attributed to the comparatively smaller spectral contribution of low energy photons at 18 MV [24, 27]. At 6 MV, the unshielded diode indicated an under-response by up to 6% for all the small field sizes that can be due to the smaller spectral contribution by low energy components for these field sizes compared to the 10×10 cm² standard reference field size [28]. However, for larger field sizes (>5×5 cm²), a reverse effect (over-response) occurred for the unshielded diode by as much as 16% due to Compton scatter photons required to be corrected in practice. On the other hand, at 18 MV the under-response correction of the unshielded diode for the same small field sizes was about 2% and the over response for the same larger field size was about 5 %, being similar to other reports done with other types of detectors [22, 24, 29].

Our results reported for the ionization chamber (Figures 6-9) were in close agreement with the K_{NR} values reported by Wulff [12] and da Rosa [30] calculated by Monte Carlo simulation. However, the increasing response estimated at MV energy ranges in our study is likely due to the relativistic density effect which affects the stopping power of water more than that of air [31, 32]. In other experiments in which TLD-100 (LiF:Mg,Ti) chips have been served as the reference detectors to observe the changes of ionization chamber responses, similar findings to ours are reported [28, 30].

The K_{NR} values measured by Scarboro et al [33] for LiF:Mg,Ti thermoluminescence detectors were obtained for a Varian linac in Houston, Texas and compared with that of a PTW31002 ionization chamber. The maximum difference of our K_{NR} calculated values with the experimental measurements reported by Scarboro et al [33] was 2%.

The unshielded diodes investigated by Dieteriche et al [34] were not the same type as those investigated by Palmans [35], which may explain the smaller K_{NR} variation found by Dieteriche et al [34]. On the other hand, Wulff [12] and da Rosa [30] investigated the same type of unshielded diode on which our calculation was based, indicating that the unshielded diodes (Figures 6-9) can well be used for the measurements of depth and lateral dose profiles of photon beams. The calibration factor for a small field size of 3×3 cm^2 reported by others [11, 28, 36, 37] has yielded a K_{NCSF} value close to unity inside the geometric field borders being similar to that estimated in this study for a small circular field size of 3 cm diameter.

Further experimental estimations of K_{NR} and K_{NCSF} values made with all the detectors used in our study indicate that EDP diode can serve well as a reference detector since very small changes of the K_{NR} and K_{NCSF} are noticed with this detector even at the peripheral regions (Figures 6-9).

Conclusion

For special small-field dosimetry, we considered small-field calibration conditions with 4×4 cm^2 field size, and the conversion factor K_{NCSF} instead of K_{NR}. Our calculations illustrated that for the restricted fields, the unshielded diodes can be used with small deviations of K_{NR} from unity similar to other reports done with TLDs. Most previous studies have calculated the correction factors for the small fields based on the common protocols (TRS398 and TG51) used for standard reference condition. However, the dosimetric parameters used in such protocols lead to significant errors when applied for small circular filed sizes having less than 30 mm diameter as experienced in this study and reported in other investigations.

Under such circumstances to reduce the effect of small changes in beam quality, implementing the correction factors measured/calculated based on the new dosimetry protocol proposed for small fields (TG155) increases the dosimetric precision and accuracy of radiotherapy procedures carried out for such field sizes.

Acknowledgment

We would like to appreciate the generous help and assistance provided by Dr. H. Nedaee and Dr. M. Yarahmadi for conducting this research. Technical assistance and access provided to the linac facilities by the staff of radiotherapy departments of Pars and Shohadaye-Tajrish Hospitals in Tehran/Iran are also greatly appreciated.

Conflict of Interest

None

References

1. Duggan DM, Coffey CW, 2nd. Small photon field dosimetry for stereotactic radiosurgery. Med Dosim. 1998;23:153-9. doi.org/10.1016/S0958-3947(98)00013-2. PubMed PMID: 9783268.
2. Ding GX, Duggan DM, Coffey CW. Commissioning stereotactic radiosurgery beams using both experimental and theoretical methods. Phys Med Biol. 2006;51:2549-66. doi.org/10.1088/0031-9155/51/10/013. PubMed PMID: 16675869.
3. Das IJ, Ding GX, Ahnesjö A. Small fields: nonequilibrium radiation dosimetry. Medical physics. 2008;35:206-15. doi.org/10.1118/1.2815356.
4. Czarnecki D, Zink K. Monte Carlo calculated correction factors for diodes and ion chambers in small photon fields. Phys Med Biol. 2013;58:2431-44. doi.org/10.1088/0031-9155/58/8/2431. PubMed PMID: 23514734.
5. Andreo P, Burns DT, Hohlfeld K, Huq MS, Kanai T, Laitano F, et al. Absorbed dose determination in external beam radiotherapy: an international code of practice for dosimetry based on standards of absorbed dose to water. IAEA TRS. 2000.
6. Almond PR, Biggs PJ, Coursey B, Hanson W, Huq MS, Nath R, et al. AAPM's TG-51 protocol for clinical reference dosimetry of high-energy photon and electron beams. Medical physics. 1999;26:1847-70. doi.org/10.1118/1.598691.
7. Kawrakow I, Rogers DW, Walters BR. Large efficiency improvements in BEAMnrc using directional bremsstrahlung splitting. Med Phys. 2004;31:2883-98. doi.org/10.1118/1.1788912.

PubMed PMID: 15543798.

8. Chofor N, Harder D, Willborn K, Ruhmann A, Poppe B. Low-energy photons in high-energy photon fields--Monte Carlo generated spectra and a new descriptive parameter. Z Med Phys. 2011;21:183-97. doi.org/10.1016/j.zemedi.2011.02.002. PubMed PMID: 21530198.
9. Alfonso R, Andreo P, Capote R, Huq MS, Kilby W, Kjall P, et al. A new formalism for reference dosimetry of small and nonstandard fields. Med Phys. 2008;35:5179-86. doi.org/10.1118/1.3005481. PubMed PMID: 19070252.
10. Kawrakow I, Rogers DW, Walters BR. Large efficiency improvements in BEAMnrc using directional bremsstrahlung splitting. Med Phys. 2004;31:2883-98. doi.org/10.1118/1.1788912. PubMed PMID: 15543798.
11. American Assiciation of Medical Physicists Task Group 155 report: Small fields and non-equilibrium condition photon beam dosimetry, AAPM, 2012. (Pre-released version of TG155 AAPM report, accessed via private communication). Available from: http://www.aapm.org/meetings/amos2/pdf/59-17153-34508-631. pdf.
12. Wulff J, Heverhagen JT, Karle H, Zink K. Investigation of correction factors for non-reference conditions in ion chamber photon dosimetry with Monte-Carlo simulations. Z Med Phys. 2010;20:25-33. doi.org/10.1016/j.zemedi.2009.09.003. PubMed PMID: 20211423.
13. Aspradakis M, Byrne J, Palmans H, Conway J, Rosser K, Warrington A, et al. IPEM report 103:'Small Field MV Photon Dosimetry'. 2010, York, UK. Institute of Physics and Engineering in Medicine (IPEM). 2010;42;42026432.
14. Ding GX, Duggan DM, Coffey CW. A theoretical approach for non-equilibrium radiation dosimetry. Phys Med Biol. 2008;53:3493-9. doi.org/10.1088/0031-9155/53/13/006. PubMed PMID: 18552420.
15. Rogers DW, Faddegon BA, Ding GX, Ma CM, We J, Mackie TR. BEAM: a Monte Carlo code to simulate radiotherapy treatment units. Med Phys. 1995;22:503-24. doi.org/10.1118/1.597552. PubMed PMID: 7643786.
16. Kawrakow I, Rogers D. The EGSnrc code system: Monte Carlo simulation of electron and photon transport. 2000.
17. Kawrakow I, Mainegra-Hing E, Tessier F, Walters B. The EGSnrc C++ class library. NRC Report PIRS-898 (rev A). 2009.
18. Rogers D, Kawrakow I, Seuntjens J, Walters B, Mainegra-Hing E. NRC user codes for EGSnrc. NRCC Report PIRS-702 (Rev. B). 2003.
19. In: German Institute of Standards, DIN 6800-2. Procedures of dosimetry with probe-type detectors for photon and electron radiation – Part 2: Dosimetry of high-energy photon and electron radiation with ionization chambers. 2008. Available from: http://www.sis.se/metrologi-och-m%C3%A4tning-fysikaliska-fenomen/str%C3%A5lningsm%C3%A4tning/din-6800-2.
20. In: German Institute of Standards, DIN 6800-5. Procedures of dosimetry with probe-type detectors for photon and electron radiation-Part 5: TLD dosimetry. 2005. Available from: http://www.din.de/en/getting-involved/standards-committees/nar/standards/wdc-beuth:din21:76603404.
21. Araki F. Monte Carlo calculations of correction factors for plane-parallel ionization chambers in clinical electron dosimetry. Med Phys. 2008;35:4033-40. doi.org/10.1118/1.2968102. PubMed PMID: 18841855.
22. Zink K, Wulff J. Beam quality corrections for parallel-plate ion chambers in electron reference dosimetry. Phys Med Biol. 2012;57:1831-54. doi.org/10.1088/0031-9155/57/7/1831. PubMed PMID: 22411097.
23. Yin Z, Hugtenburg RP, Beddoe AH. Response of silicon diode dosemeters to scattered radiation from megavoltage photon beams. Radiat Prot Dosimetry. 2002;101:415-8. doi.org/10.1093/oxfordjournals.rpd.a006014. PubMed PMID: 12382780.
24. Eklund K, Ahnesjo A. Spectral perturbations from silicon diode detector encapsulation and shielding in photon fields. Med Phys. 2010;37:6055-60. doi.org/10.1118/1.3501316. PubMed PMID: 21158317.
25. Edwards CR, Mountford PJ, Green S, Palethorpe JE, Moloney AJ. The low energy X-ray response of the LiF:Mg:Cu:P thermoluminescent dosemeter: a comparison with LiF:Mg:Ti. Br J Radiol. 2005;78:543-7. doi.org/10.1259/bjr/73133162. PubMed PMID: 15900061.
26. Muir BR, McEwen MR, Rogers DW. Measured and Monte Carlo calculated K(Q) factors: accuracy and comparison. Med Phys. 2011;38:4600-9. doi.org/10.1118/1.3600697. PubMed PMID: 21928633.
27. Hultqvist M, Fernandez-Varea JM, Izewska J. Monte Carlo simulation of correction factors for IAEA TLD holders. Phys Med Biol. 2010;55:N161-6. doi.org/10.1088/0031-9155/55/6/N03.
28. Konnai A, Nariyama N, Ohnishi S, Odano N.

Energy response of LiF and Mg2SiO4 TLDs to 10-150 keV monoenergetic photons. Radiat Prot Dosimetry. 2005;115:334-6. doi.org/10.1093/rpd/nci166. PubMed PMID: 16381741.

29. Cranmer-Sargison G, Weston S, Evans JA, Sidhu NP, Thwaites DI. Implementing a newly proposed Monte Carlo based small field dosimetry formalism for a comprehensive set of diode detectors. Med Phys. 2011;38:6592-602. doi.org/10.1118/1.3658572. PubMed PMID: 22149841.
30. da Rosa LA, Cardoso SC, Campos LT, Alves VG, Batista DV, Facure A. Percentage depth dose evaluation in heterogeneous media using thermoluminescent dosimetry. J Appl Clin Med Phys. 2010;11:2947. PubMed PMID: 20160687.
31. Scott AJ, Nahum AE, Fenwick JD. Using a Monte Carlo model to predict dosimetric properties of small radiotherapy photon fields. Med Phys. 2008;35:4671-84. doi.org/10.1118/1.2975223. PubMed PMID: 18975713.
32. Yarahmadi M, Allahverdi M, Nedaie HA, Asnaashari K, Vaezzadeh SA, Sauer OA. Improvement of the penumbra for small radiosurgical fields using flattening filter free low megavoltage beams. Z Med Phys. 2013;23:291-9. doi.org/10.1016/j.zemedi.2013.03.011. PubMed PMID: 23669174.
33. Scarboro SB, Followill DS, Howell RM, Kry SF. Variations in photon energy spectra of a 6 MV beam and their impact on TLD response. Med Phys. 2011;38:2619-28. doi.org/10.1118/1.3575419. PubMed PMID: 21776799.
34. Dieterich S, Sherouse GW. Experimental comparison of seven commercial dosimetry diodes for measurement of stereotactic radiosurgery cone factors. Med Phys. 2011;38:4166-73. doi.org/10.1118/1.3592647. PubMed PMID: 21859018.
35. Palmans H. Determination of the beam quality index of high-energy photon beams under nonstandard reference conditions. Med Phys. 2012;39:5513-9. doi.org/10.1118/1.4745565. PubMed PMID: 22957618.
36. Scott AJ, Nahum AE, Fenwick JD. Using a Monte Carlo model to predict dosimetric properties of small radiotherapy photon fields. Med Phys. 2008;35:4671-84. doi.org/10.1118/1.2975223. PubMed PMID: 18975713.
37. Sauer OA, Wilbert J. Functional representation of tissue phantom ratios for photon fields. Med Phys. 2009;36:5444-50. doi.org/10.1118/1.3250867. PubMed PMID: 20095257.